

正极材料 $\text{Li}(\text{Ni}_{0.5}\text{Mn}_{0.5})_{1-x}\text{M}_x\text{O}_2$ ($\text{M}=\text{Ti}, \text{Al}; x=0, 0.02$) 电化学行为的比较研究

曹四海 王志兴* 李新海 吕 莹 郭华军 彭文杰
(中南大学冶金科学与工程学院, 长沙 410083)

关键词: 锂离子电池; $\text{LiNi}_{0.5}\text{Mn}_{0.5}\text{O}_2$; 掺杂; 固相法

中图分类号: O614.11

文献标识码: A

文章编号: 1001-4861(2006)08-1540-05

Comparative Study on Electrochemical Behavior of $\text{Li}(\text{Ni}_{0.5}\text{Mn}_{0.5})_{1-x}\text{M}_x\text{O}_2$ ($\text{M}=\text{Ti}, \text{Al}; x=0, 0.02$) Cathode Materials

CAO Si-Hai WANG Zhi-Xing* LI Xin-Hai LU Ying GUO Hua-Jun PENG Wen-Jie
(School of Metallurgical Science and Engineering, Central South University, Changsha 410083)

Abstract: Layered $\text{Li}(\text{Ni}_{0.5}\text{Mn}_{0.5})_{1-x}\text{M}_x\text{O}_2$ ($\text{M}=\text{Ti}, \text{Al}; x=0, 0.02$) cathode materials for lithium-ion batteries were synthesized by one step solid-state method using $\text{Ni}(\text{OH})_2$, MnCO_3 , Li_2CO_3 , TiO_2 and $\text{Al}(\text{OH})_3$ as starting materials. The effect of Ti and Al doping on the structure and electrochemical performance of $\text{Li}(\text{Ni}_{0.5}\text{Mn}_{0.5})_{1-x}\text{M}_x\text{O}_2$ ($\text{M}=\text{Ti}, \text{Al}; x=0, 0.02$) has been investigated. $\text{LiNi}_{0.5}\text{Mn}_{0.5}\text{O}_2$, $\text{Li}(\text{Ni}_{0.5}\text{Mn}_{0.5})_{0.98}\text{Ti}_{0.02}\text{O}_2$ and $\text{Li}(\text{Ni}_{0.5}\text{Mn}_{0.5})_{0.98}\text{Al}_{0.02}\text{O}_2$ delivered $149 \text{ mAh} \cdot \text{g}^{-1}$, $160 \text{ mAh} \cdot \text{g}^{-1}$, $164 \text{ mAh} \cdot \text{g}^{-1}$, respectively, at a current of $20 \text{ mA} \cdot \text{g}^{-1}$ between 2.5 V and 4.3 V at room temperature, and remained 86%, 91%, 91% of the initial discharge capacity respectively after 30 cycles. AC impedance studies show that Ti and Al doping in $\text{Li}(\text{Ni}_{0.5}\text{Mn}_{0.5})_{1-x}\text{M}_x\text{O}_2$ ($\text{M}=\text{Ti}, \text{Al}; x=0, 0.02$) decreased the resistance of charge transfer R_{ct} of cathode materials.

Key words: lithium-ion battery; $\text{LiNi}_{0.5}\text{Mn}_{0.5}\text{O}_2$; doping; solid-state method

0 Introduction

Many efforts have been made to develop new materials as an alternative to LiCoO_2 due to the relatively high cost and toxicity of Co. Much attention has been paid to layered structure cathode materials such as LiMnO_2 and LiNiO_2 due to their lower cost and larger capacity compared with LiCoO_2 . However, LiNiO_2 has severe problems associated with the preparation of phase-pure material, multi-phase reac-

tion during charge process, and thermal instability in organic electrolytes in charged state^[1]. And layered structure LiMnO_2 was observed to undergo a detrimental phase transformation to spinel phase, which led to poor cycling performance^[2]. Since Ohzuku et al.^[3] successfully synthesized $\text{LiNi}_{0.5}\text{Mn}_{0.5}\text{O}_2$ with excellent electrochemical performance by solid state method at 1000°C , $\text{LiNi}_{0.5}\text{Mn}_{0.5}\text{O}_2$ has attracted much attention from researchers in view of its high reversible capacity, high thermal stability, lower cost and less toxicity.

收稿日期:2006-02-20。收修改稿日期:2006-05-18。

中南大学博士后基金资助项目。

*通讯联系人。E-mail:zxwang@mail.csu.edu.cn

第一作者:曹四海,男,25岁,硕士研究生;研究方向:新型能源材料及化学电源。

XPS studies show that the transition metal elements are predominantly in Ni^{2+} and Mn^{4+} oxidation state and about 6%~8% of Ni- and Mn-ions in the compound are in mixed valence state due to the dynamic ion-equilibrium, $\text{Ni}^{2+} + \text{Mn}^{4+} \rightarrow \text{Ni}^{3+} + \text{Mn}^{3+}$ [4]. Ni and Mn K-edge X-ray absorption near-edge structure (XANES) results on $\text{LiNi}_{0.5}\text{Mn}_{0.5}\text{O}_2$ are also in agreement with results by Johnson et al. [5]. A two-electron redox reaction ($\text{Ni}^{2+} \rightarrow \text{Ni}^{4+}$) is assumed for the charge-discharge process and confirmed by XANES up to 4.2 V in $\text{LiNi}_{0.5}\text{Mn}_{0.5}\text{O}_2$ [4-6].

In the previous study we have synthesized layered structure $\text{LiNi}_{0.5}\text{Mn}_{0.5}\text{O}_2$ cathode material using $\text{Ni}(\text{OH})_2$, MnCO_3 and Li_2CO_3 as starting materials by one step solid-state reaction. However its electrochemical performance is still expected to be improved. Foreign metal ions doping has been regarded as an effective way to improve the electrochemical performance of cathode materials for lithium-ion batteries. Kang et al. [7] reported that doping of Al, Ti and Co increased discharge capacity and electronic conductivity of $\text{LiNi}_{0.5}\text{Mn}_{0.5}\text{O}_2$. Kim et al. [8] found that non-electrochemical active component Li_2TiO_3 could contribute to the stabilization of layered structure in $\text{LiNi}_{0.5}\text{Mn}_{0.5}\text{O}_2$ and could increase the columbic efficiency during the charge-discharge process. Park et al. [9] found that Al^{3+} doping on $\text{Li}[\text{Li}_{0.15}\text{Ni}_{(0.275-x/2)}\text{Al}_x\text{Mn}_{(0.575-x/2)}]\text{O}_2$ synthesized by sol-gel could prevent from the structural degradation of the electrode material and decrease the area specific impedance. Therefore the electrochemical performance of $\text{LiNi}_{0.5}\text{Mn}_{0.5}\text{O}_2$ may be improved through Ti^{4+} , Al^{3+} doping by one step solid-state method. In the present study, $\text{Li}(\text{Ni}_{0.5}\text{Mn}_{0.5})_{1-x}\text{M}_x\text{O}_2$ ($\text{M}=\text{Ti}, \text{Al}; x=0, 0.02$) cathode materials were synthesized by one step solid-state reaction, and the electrochemical behavior of $\text{Li}(\text{Ni}_{0.5}\text{Mn}_{0.5})_{1-x}\text{M}_x\text{O}_2$ ($\text{M}=\text{Ti}, \text{Al}; x=0, 0.02$) cathode materials between 2.5 V and 4.3 V at room temperature were comparatively studied.

1 Experimental

$\text{Ni}(\text{OH})_2$, MnCO_3 , Li_2CO_3 , TiO_2 and $\text{Al}(\text{OH})_3$ in stoichiometric amount were thoroughly mixed and grounded for 6 h using a ball-milling machine. The

grounded powder was heated at 800 °C for 36 h in air and then naturally cooled to room temperature in furnace.

Powder X-Ray diffraction analysis was performed on Rigaku Rint-2000 equipped with a $\text{Cu } K\alpha_1$ radiation source ($\lambda = 0.154\ 06\ \text{nm}$) and a graphite monochromator, with high voltage of 40 kV and current of 250 mA. Finely divided silicon powder was used as an internal standard. The scan was carried out in the range $10^\circ \leq 2\theta \leq 90^\circ$ at a 0.02° step and 10 s dwell-time.

Scanning electron microscope (SEM) study of the powders was performed on JEOL JSM-5600LV electron microscope with high voltage of 20 kV.

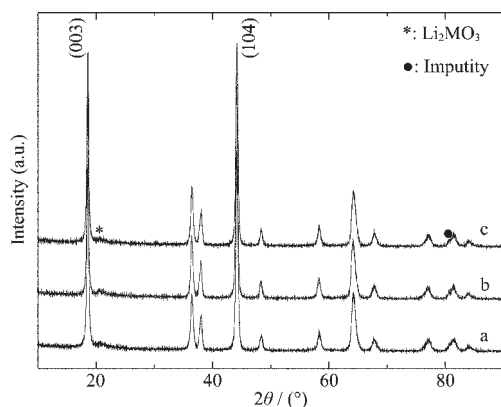
The charge/discharge tests were carried out using the CR2025 coin-type cell, which consists of a cathode and lithium metal anode separated by a Celgard 2400 porous polypropylene film with the electrolyte of $1\ \text{mol}\cdot\text{L}^{-1}$ LiPF_6 in $\text{EC}+\text{DMC}+\text{EMC}(1:1:1, \text{V/V/V})$. The positive electrode was consisted of 80wt% active material, 10wt% acetylene black and 10wt% PVDF. The mixture was thoroughly mixed, then painted on an aluminum film and dried at 120 °C for 12 h under vacuum. The cells were assembled in a glove box filled with dry argon gas. Cells were first charged to 4.3 V at a rate of $20\ \text{mA}\cdot\text{g}^{-1}$ and held for 2 h under 4.3 V, then discharged to 2.5 V at a rate of $20\ \text{mA}\cdot\text{g}^{-1}$ at room temperature.

AC Impedance measurement was carried out by means of tri-electrode cell using lithium metal as counter and reference electrodes. Cells at discharged state or charged state were stood for 8 h before AC impedance measurement and then operated between 0.001 Hz and 100 000 Hz.

2 Results and discussion

The XRD patterns of synthesized $\text{Li}(\text{Ni}_{0.5}\text{Mn}_{0.5})_{1-x}\text{M}_x\text{O}_2$ ($\text{M}=\text{Ti}, \text{Al}; x=0, 0.02$) are shown in Fig.1. All diffraction peaks can be indexed as a hexagonal α - NaFeO_2 structure with a space group of $R\bar{3}m$ the weak diffraction peaks marked with * and black circle. The peaks between 20° and 25° are caused by superlattice ordering of the Li, Ni and Mn in the 3a site, which

indicates a layered structure with Li_2MnO_3 character^[10,11]. According to literature^[12], Li_2MnO_3 contributes to the stabilization of layered structure in $\text{LiNi}_{0.5}\text{Mn}_{0.5}\text{O}_2$ during cycling process. The lattice parameters of the synthesized samples are shown in Table 1. It can be seen that for the lattice parameters of $\text{Li}(\text{Ni}_{0.5}\text{Mn}_{0.5})_{0.98}\text{Ti}_{0.02}\text{O}_2$, a and c show slight change compared with those of $\text{LiNi}_{0.5}\text{Mn}_{0.5}\text{O}_2$. This relates to the partial substitution of Ni^{2+} ($r=0.069$ nm) and Mn^{4+} ($r=0.053$ nm) by small amount of Ti^{4+} ($r=0.068$ nm). The ratio of c/a also increases and they are both above 4.936, which is in good agreement with layered structure character^[13]. For $\text{Li}(\text{Ni}_{0.5}\text{Mn}_{0.5})_{0.98}\text{Al}_{0.02}\text{O}_2$, the lattice parameter a does not change, but c shrinks clearly. This relates to the decrease of interlamellar distance of transition metals due to the substitution of Ni^{2+} ($r=0.069$ nm) and Mn^{4+} ($r=0.053$ nm) by Al^{3+} ($r=0.053$ 5 nm). The decreasing ratio of c/a suggests that the degree of layered structure decreases. The intensity ratio of I_{003}/I_{104} in $\text{Li}(\text{Ni}_{0.5}\text{Mn}_{0.5})_{0.98}\text{M}_{0.02}\text{O}_2$ materials shows some increase, which demonstrates that the degree of cation mixing in $\text{Li}(\text{Ni}_{0.5}\text{Mn}_{0.5})_{1-x}\text{M}_x\text{O}_2$ ($\text{M}=\text{Ti}, \text{Al}; x=0, 0.02$) becomes less severe^[14].



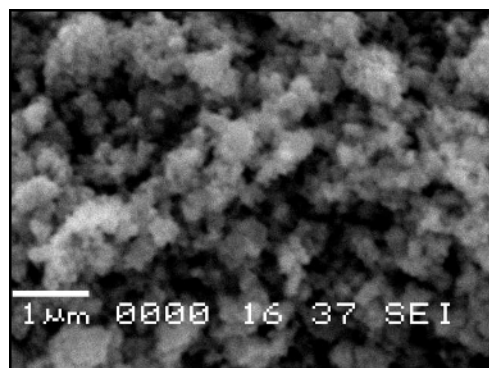
a: $\text{LiNi}_{0.5}\text{Mn}_{0.5}\text{O}_2$; b: $\text{Li}(\text{Ni}_{0.5}\text{Mn}_{0.5})_{0.98}\text{Ti}_{0.02}\text{O}_2$;
c: $\text{Li}(\text{Ni}_{0.5}\text{Mn}_{0.5})_{0.98}\text{Al}_{0.02}\text{O}_2$

Fig.1 XRD patterns of $\text{Li}(\text{Ni}_{0.5}\text{Mn}_{0.5})_{1-x}\text{M}_x\text{O}_2$ ($\text{M}=\text{Ti}, \text{Al}; x=0, 0.02$)

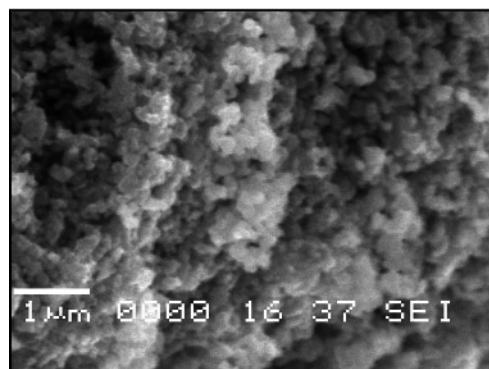
Table 1 Lattice parameters of $\text{Li}(\text{Ni}_{0.5}\text{Mn}_{0.5})_{1-x}\text{M}_x\text{O}_2$ ($\text{M}=\text{Ti}, \text{Al}; x=0, 0.02$)

$\text{Li}(\text{Ni}_{0.5}\text{Mn}_{0.5})_{1-x}\text{M}_x\text{O}_2$	a / nm	c / nm	c/a	I_{003}/I_{103}
$x=0$	0.288 5	1.424 2	4.937	0.962
$\text{Ti}(x=0.02)$	0.288 4	1.424 3	4.939	1.017
$\text{Al}(x=0.02)$	0.288 5	1.419 6	4.920	0.972

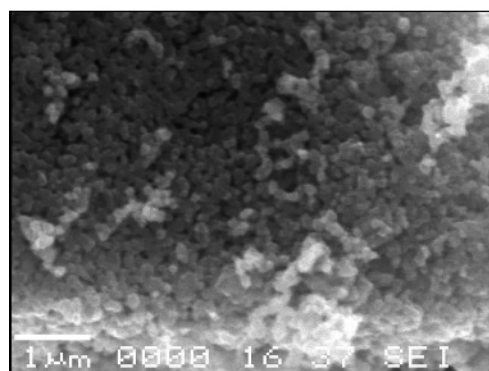
The SEM photographs of the samples are shown in Fig.2. It can be seen that the particles of all three samples are distributed homogeneously. The average size of particles in all samples is less than 150 nm. In addition, doping small amount of Ti^{4+} and Al^{3+} reduced the agglomeration of particles.



A: $\text{LiNi}_{0.5}\text{Mn}_{0.5}\text{O}_2$



B: $\text{Li}(\text{Ni}_{0.5}\text{Mn}_{0.5})_{0.98}\text{Ti}_{0.02}\text{O}_2$

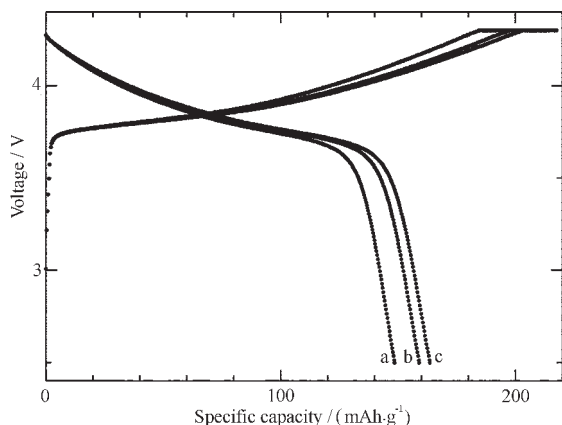


C: $\text{Li}(\text{Ni}_{0.5}\text{Mn}_{0.5})_{0.98}\text{Al}_{0.02}\text{O}_2$

Fig.2 SEM photographs of $\text{Li}(\text{Ni}_{0.5}\text{Mn}_{0.5})_{1-x}\text{M}_x\text{O}_2$ ($\text{M}=\text{Ti}, \text{Al}; x=0, 0.02$)

The charge-discharge curves of the first cycle for the synthesized samples are shown in Fig.3. Between 2.5 V and 4.3 V, $\text{LiNi}_{0.5}\text{Mn}_{0.5}\text{O}_2$, $\text{Li}(\text{Ni}_{0.5}\text{Mn}_{0.5})_{0.98}\text{Ti}_{0.02}\text{O}_2$, $\text{Li}(\text{Ni}_{0.5}\text{Mn}_{0.5})_{0.98}\text{Al}_{0.02}\text{O}_2$ delivered $149 \text{ mAh} \cdot \text{g}^{-1}$, 160

$\text{mAh} \cdot \text{g}^{-1}$, $164 \text{ mAh} \cdot \text{g}^{-1}$, respectively, at a current of $20 \text{ mA} \cdot \text{g}^{-1}$ at room temperature. The coulomb efficiency of the first cycle for the above three samples is 75%, 81%, 83%, respectively. It's obvious that doping Ti^{4+} and Al^{3+} improved the electrochemical performance of $\text{LiNi}_{0.5}\text{Mn}_{0.5}\text{O}_2$.



a: $\text{LiNi}_{0.5}\text{Mn}_{0.5}\text{O}_2$; b: $\text{Li}(\text{Ni}_{0.5}\text{Mn}_{0.5})_{0.98}\text{Ti}_{0.02}\text{O}_2$;

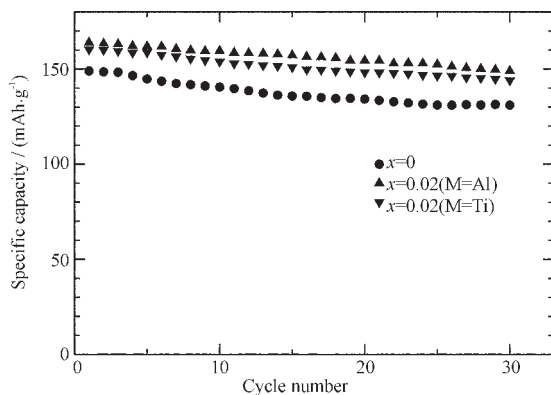
c: $\text{Li}(\text{Ni}_{0.5}\text{Mn}_{0.5})_{0.98}\text{Al}_{0.02}\text{O}_2$

Test conditions: charge/discharge rate $20 \text{ mA} \cdot \text{g}^{-1}$,

voltage range 2.5 V~4.3 V, room temperature

Fig.3 Charge-discharge curves of $\text{Li}(\text{Ni}_{0.5}\text{Mn}_{0.5})_{1-x}\text{M}_x\text{O}_2$ ($\text{M}=\text{Ti}, \text{Al}; x=0, 0.02$) in the first cycle

The cycling performance of the samples is shown in Fig.4. After 30 cycles at a current of $20 \text{ mA} \cdot \text{g}^{-1}$ between 2.5 V and 4.3 V, $\text{LiNi}_{0.5}\text{Mn}_{0.5}\text{O}_2$, $\text{Li}(\text{Ni}_{0.5}\text{Mn}_{0.5})_{0.98}\text{Ti}_{0.02}\text{O}_2$, $\text{Li}(\text{Ni}_{0.5}\text{Mn}_{0.5})_{0.98}\text{Al}_{0.02}\text{O}_2$ remained 86%, 91%, 91% of the initial discharge capacity respectively. The cycling performance of the samples was improved after doping Ti^{4+} and Al^{3+} . This maybe relate to improved



Test conditions: charge/discharge rate $20 \text{ mA} \cdot \text{g}^{-1}$,

Voltage range 2.5 V~4.3 V, room temperature

Fig.4 Cycling curves of $\text{Li}(\text{Ni}_{0.5}\text{Mn}_{0.5})_{1-x}\text{M}_x\text{O}_2$ ($\text{M}=\text{Ti}, \text{Al}; x=0, 0.02$)

stabilization of electrode materials and the increase of electrical conductivity of samples through doping Ti^{4+} and Al^{3+} . In addition, Li_2TiO_3 decreased the activity of the surface of electrode at charged state for $\text{Li}(\text{Ni}_{0.5}\text{Mn}_{0.5})_{0.98}\text{Ti}_{0.02}\text{O}_2$, which contributes to the improved cycling performance^[15].

The impedance spectra of the electrode materials at full discharged and charged state are shown in Fig. 5A and 5B, respectively. And the equivalent circuit used for fitting the impedance spectra is shown in Fig. 6. In Fig.5A, the impedance spectra are consisted of one semicircle in high-frequency range and a line inclined at constant angle to the real axis in the low-frequency range. The semicircle should be attributed to surface film on the active material (R_{sf} , surface film resistance)^[16,17] and the inclined line is attributed to Warburg impedance associated with lithium ion diffusion through the cathode^[13]. The impedance spectra of the materials charged to 4.5 V are shown in Fig.5B. Different from those of discharged state, the impedance spectra consists of two semicircles in high-

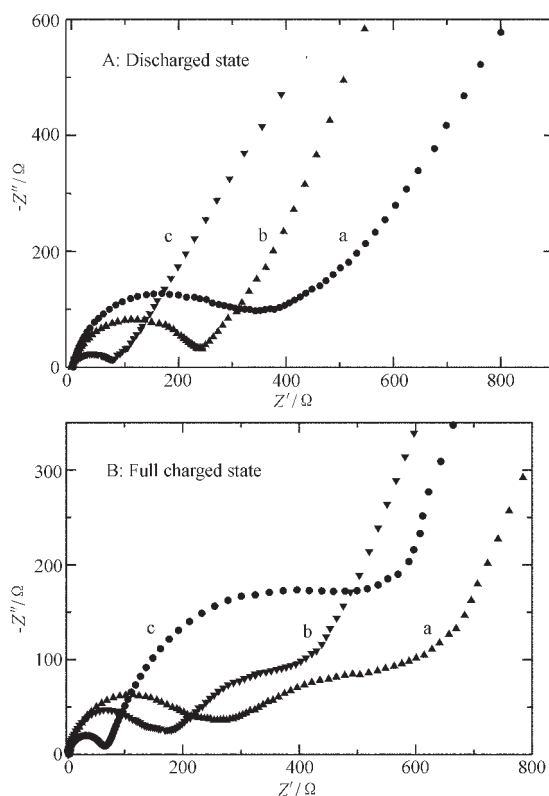
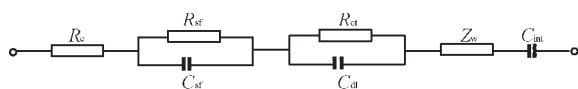


Fig.5 AC impedance spectra of $\text{Li}(\text{Ni}_{0.5}\text{Mn}_{0.5})_{1-x}\text{M}_x\text{O}_2$ ($\text{M}=\text{Ti}, \text{Al}; x=0, 0.02$)



R_e : resistance of electrolyte;

R_{sf} : surface film resistance;

C_{sf} : capacitance associated surface film;

R_{ct} : charge transfer resistance;

C_{dl} : double layer capacitance;

Z_w : Warburg impedance associated with lithium ion diffusion through the cathode;

C_{int} : Li^+ intercalation capacitance;

Fig.6 Equivalent circuit used for fitting the impedance spectra

and intermediate-frequency range and a line inclines at constant angle to the real axis in the low-frequency range. The second semicircle should be attributed to R_{ct} , resistance of charge transfer at the electrode-electrolyte interface. From discharged state to charged state, the decrease of R_{sf} is obvious because the inactive surface film covering the virgin electrode surface is destructed or modified by the current flux. The result is in good agreement with other report^[17]. In addition, doping of Ti^{4+} and Al^{3+} reduced AC impedance evidently no matter the system was at discharged or charged state, thus resulting in the improvement of electric conductivity of materials. The decrease of impedance and the increase of electrical conductivity of samples through doping foreign metal ions^[7] should be the main reason for the increase in discharge capacity of $\text{Li}(\text{Ni}_{0.5}\text{Mn}_{0.5})_{0.98}\text{M}_{0.02}\text{O}_2$ ($\text{M}=\text{Ti}, \text{Al}$). From this point the effect for doping of Al^{3+} is more obvious than that for doping of Ti^{4+} . This will then improve the electrochemical performance of materials, which agrees well with the electrochemical results in Fig.3 and Fig.4.

3 Conclusions

Layered $\text{Li}(\text{Ni}_{0.5}\text{Mn}_{0.5})_{1-x}\text{M}_x\text{O}_2$ ($\text{M}=\text{Ti}, \text{Al}$; $x=0, 0.02$) cathode materials for lithium ion batteries were synthesized at 800 °C for 36 h by one step solid-state method using $\text{Ni}(\text{OH})_2$, MnCO_3 , Li_2CO_3 , TiO_2 and $\text{Al}(\text{OH})_3$ as starting materials. XRD results show that synthesized $\text{Li}(\text{Ni}_{0.5}\text{Mn}_{0.5})_{1-x}\text{M}_x\text{O}_2$ ($\text{M}=\text{Ti}, \text{Al}$; $x=0, 0.02$) have layered structure with space group of $R\bar{3}m$. Electrochemical tests at room temperature demonstrate that

synthesized samples $\text{LiNi}_{0.5}\text{Mn}_{0.5}\text{O}_2$, $\text{Li}(\text{Ni}_{0.5}\text{Mn}_{0.5})_{0.98}\text{Ti}_{0.02}\text{O}_2$ and $\text{Li}(\text{Ni}_{0.5}\text{Mn}_{0.5})_{0.98}\text{Al}_{0.02}\text{O}_2$ delivered $149 \text{ mAh} \cdot \text{g}^{-1}$, $160 \text{ mAh} \cdot \text{g}^{-1}$, $164 \text{ mAh} \cdot \text{g}^{-1}$ between 2.5 V and 4.3 V at a current of $20 \text{ mA} \cdot \text{g}^{-1}$, and remained 86%, 91%, 91% of the initial discharge capacity, respectively, after 30 cycles. Impedance study indicate that the resistance of charge transfer R_{ct} of materials decreased obviously after doping Ti^{4+} and Al^{3+} . High capacity and improved cycling performance should be attributed to the increase of electric conductivity of $\text{Li}(\text{Ni}_{0.5}\text{Mn}_{0.5})_{0.98}\text{M}_{0.02}\text{O}_2$ ($\text{M}=\text{Ti}, \text{Al}$) cathode materials.

References:

- [1] Hirano A, Kanno R, Kawamoto Y, et al. *Solid State Ionics*, **1995**,**78**:123~131
- [2] Amundsen B, Desilvestro J, Groutso T, et al. *J. Electrochem. Soc.*, **2000**,**147**:4078~4082
- [3] Ohzuku T, Makimura Y. *Chem. Lett.*, **2001**,**8**:744~745
- [4] Shaju K M, Rao G V S, Chowdari B V R. *Electrochim. Acta*, **2003**,**48**:1505~1514
- [5] Johnson C S, Kim J S, Kropf A J, et al. *Electrochem. Commun.*, **2002**,**4**:492~498
- [6] Yoon W S, Paik Y, Yang X Q, et al. *Electrochem. Solid-State Lett.*, **2002**,**5**:A263~A266
- [7] Kang S H, Kim J, Stoll M E, et al. *J. Power Sources*, **2002**, **112**:41~48
- [8] Kim J S, Johnson C S, et al. *Electrochem. Commun.*, **2002**,**4**: 205~209;
- [9] Park S H, Sun Y K. *J. Power Sources*, **2003**,**119~121**:161~165
- [10] Lu Z H, Beaulieu L Y, Donabarger R A, et al. *J. Electrochem. Soc.*, **2002**,**149**:A778~A791
- [11] Lu Z H, Dahn J R. *J. Electrochem. Soc.*, **2003**,**150**:A1044~A1051
- [12] Kim J H, Sun Y K. *J. Power Sources*, **2003**,**119~121**:166~170
- [13] Kim J H, Park C W, Sun Y K. *Solid State Ionics*, **2003**,**164**: 43~49
- [14] Ohzuku T, Ueda A, Nagayama M. *J. Electrochem. Soc.*, **1993**,**140**:1862~1870
- [15] Johnson C S, Kim J S, Kropf A J, et al. *J. Power Sources*, **2003**,**119~121**:139~144
- [16] Dokko K, Mohamedi M, Fujita Y. et al. *J. Electrochem. Soc.*, **2001**,**148**:A422~A426
- [17] Shaju K M, Rao G V S, Chowdari B V R. *Electrochim. Acta*, **2003**,**49**:1565~1576